

**STAINLESS STEEL WORLD CONFERENCE**  
**1999**

Paper No. P99006

A MODEL FOR CORROSION OF THE DEPLETED ZONES  
AROUND SIGMA PRECIPITATES PRODUCED DURING WELDING  
OF SUPER DUPLEX STAINLESS STEEL

R FRANCIS, G R WARBURTON

Weir Materials & Foundries  
Park Works  
Newton Heath  
Manchester  
M40 2BA  
United Kingdom

**A B S T R A C T**

Super duplex stainless steel has now been in service since 1989, with well over 1 million welds, and generally few problems have occurred. However, during welding, particularly of small diameter thin walled pipe, it is possible for small amounts of sigma phase to be precipitated in the low temperature heat affected zone. The depletion of chromium and molybdenum around the precipitates reduces the local corrosion resistance, and the question that is frequently asked is, how much sigma phase can be tolerated before corrosion resistance is significantly impaired?

In the paper a simple model is presented for the depleted zone around sigma precipitates produced during the welding of Zeron 100 super duplex stainless steel. The requirements for corrosion to propagate are evaluated, and the precipitate size is shown to be the most critical factor. The tolerable level of sigma phase is shown to vary hugely with particle diameter.

Using typical precipitate sizes found in Zeron 100, the model's predictions are shown to correlate well with the results of corrosion tests of welds in chlorinated sea water. Similar results are found for sour oil and gas process brines and flue gas desulphurisation slurries.

The results of the modelling exercise have important implications for engineering fabrication of super duplex stainless steels. Because of the dramatic influence of precipitate size there is no single figure for the tolerable level of sigma phase which is acceptable. It is concluded that fitness for purpose tests for welds are more relevant than metallography and counting of sigma particles.

**KEYWORDS:-** Super duplex stainless steel, welding, sigma phase, corrosion.

## 1.0 INTRODUCTION

Zeron 100 super duplex stainless steel has been in service in the wrought form since 1989. It has been calculated that in the ten years since then at least 1 million welds have entered service. Largely these have given excellent service, but occasionally problems are experienced with corrosion. This usually happens when a weld qualification procedure fails to pass an ASTM G48A corrosion test in ferric chloride. A microstructural examination of these samples usually reveals that sigma phase has precipitated, most often in the low temperature heat affected zone. The problem is frequently cured by repeating the weld qualification at lower heat inputs and/or lower interpass temperatures.

One question which is often asked, but to which there is currently no answer, is "what is the critical concentration of sigma phase to give cause for concern over corrosion resistance?" This report presents a simple mathematical model which attempts to predict this and compare the results with available corrosion data.

## 2.0 SIGMA PHASE

Sigma phase is an intermetallic, rich in chromium and molybdenum compared to the base metal composition. It is formed when the alloy is cooled slowly in the temperature range 1000°C to 750 °C, as shown in Figure 1, taken from reference 1.

Many tests on sigma phase precipitation have been carried out by isothermal heat treatment in the above temperature range, but, in welding, sigma precipitates in material experiencing a constantly varying thermal cycle with concurrent strain from local expansion and contraction. Most welding operations are multipass, which further complicates simulation of the precipitation kinetics. Nevertheless, the key point is that sigma forms when the cooling time, usually given from 1200°C to 800°C, is too long.

One of the main differences between isothermally produced sigma phase and that from welding operations is size. This was reported by Francis (2), who observed a sigma particle diameter of 1 to 2µm from welding and 10 to 15µm diameter from isothermal heat treatment. The results of many observations in the WM&F laboratory since that time suggests that isothermally produced sigma particles are 3 to 7 times larger than those from welding cycles. As the time at elevated temperature is increased more sigma particles nucleate and existing sigma particles grow. The importance of this is discussed in a later section.

A number of workers have measured the composition of sigma phase, as shown in Table 1. The typical base metal composition is Fe/25 Cr/3Mo/6Ni. The increased concentrations of chromium and molybdenum in the sigma phase over the base metal composition means that the matrix surrounding the sigma precipitates must be depleted in these elements. The resistance of stainless steels to localised attack in brines is dependent principally on the elements, chromium, molybdenum and nitrogen. These are often combined into the Pitting Resistance Equivalent Number (PREN) Where:-

$$\text{PREN} = \% \text{ Cr} + 3.3\% \text{ Mo} + 16\% \text{ N}.$$

This formula is empirical but it gives a guide to the relative effect of these elements. Zeron 100 has a guaranteed PREN > 40, but a decrease locally of PREN to, say, 34 can give rise to corrosion in many environments. As sigma phase precipitates from the ferrite phase, which contains very little nitrogen, it has been assumed that there is also no nitrogen in the sigma phase for the PREN evaluations in Table. 1.

The lowering of the PREN of the material around the sigma particle clearly creates a depleted zone of reduced corrosion resistance. In the following section the scale and extent of this will be modelled.

### **3.0 EVOLUTION OF THE DEPLETED ZONE**

#### **3.1 Diffusion**

The extent of the depleted zone around a sigma particle will depend on the ability of chromium and molybdenum to diffuse from the bulk material to the particle during its growth. For this a number of factors need to be calculated. The first of these are the diffusion coefficients of chromium and molybdenum. Table 2 presents some data taken from Kaur & Gust (12). The temperature is clearly a critical parameter. In a welding cycle the critical time ( $\Delta T$ ) is the cooling time from 1200°C to 800°C, but during this cycle most of the time will be spent at lower temperatures i.e. the rate of cooling decreases as the temperature decreases. Hence a figure of ~ 900°C has arbitrarily been chosen as being typical during cooling.

This is supported by some recent work at TWI (13). Materials heat treated at 1000°C to produce 1.4% intermetallics showed no loss in the critical pitting temperature (CPT) in the ASTM G48A ferric chloride test, while treatment at 800°C to produce the same sigma content showed a 30°C reduction in CPT. This is believed to be because chromium and molybdenum are more mobile at higher temperatures and hence diffusion to provide the extra chromium and molybdenum in the precipitate can occur over a wider area around the site of precipitation. This means the localised reduction in corrosion resistance is much less than that around precipitates produced at lower temperatures.

Classically sigma phase precipitates from the ferrite phase, although in duplex stainless steel it is usually found at the ferrite-austenite phase boundaries. Recent, unpublished work from TWI suggests that pit initiation is often in the austenite adjacent to the sigma particle, although it usually spreads quickly to the ferrite. This could be because some of the chromium and molybdenum to form the sigma particle has come from the austenite. Diffusion in austenite is much slower than in ferrite (c.f. Table 2) and hence any depleted zone in the austenite will be very narrow. However, this narrowness may also mean that its corrosion resistance is reduced more than that of the ferrite and, hence, the austenitic depleted zone becomes the favoured site of attack. As the depleted zone in the ferrite will be more extensive, the propagation of corrosion will be largely controlled by the degree and extent of the depletion in the ferrite. Hence diffusion coefficients in the ferrite phase are considered for this preliminary study of precipitation. It is clear that this whole area of intermetallic formation would benefit from further, detailed study.

The width of chromium depleted zones when chromium carbides are precipitated at grain boundaries was treated by Strawström and Hillert (14). As sigma particles are precipitated from the ferrite phase at the phase boundary in duplex stainless steels, a similar one dimensional treatment can be used. They showed the width of the depleted zone ( $w$ ) was given by

$$w = 2 \sqrt{Dt} \quad \left\{ \frac{Cr_p - Cr_i}{Cr_o - Cr_i} \right\}$$

where  $D$  = diffusion coefficient  
 $t$  = time  
 $Cr_o$  = bulk chromium concentration  
 $Cr_i$  = chromium concentration at the carbide interface  
 $Cr_p$  = chromium concentration for loss of passivity

This treatment assumes a thin continuous carbide phase, but it can be regarded as valid also for the precipitation of intermetallics. Using some estimated values for the Cr term a value close to 1 was generally found. Hence a value of 1 was used in all subsequent calculations for simplicity. Table 3 shows the calculated depleted zone widths for a range of diffusion coefficients from Table 2, and times from 10 to 240 seconds.

A time of 60 seconds at 900°C (diffusion coefficient  $\approx 1.0 \text{ E-}15 \text{ m}^2/\text{sec}$ ) gives a calculated depleted zone width of  $\sim 0.5 \mu\text{m}$ . However, Figure 1 suggests that 60 seconds at 900°C should not result in sigma precipitation. Charles (15) showed that, for commercially produced super duplex stainless steels, the time for sigma precipitation can decrease to about 150 seconds at 900°C. Unpublished work at WM&F has shown that, during welding, a delta T of 60 seconds is about the safe maximum.

The reason for this reduction is two fold. Firstly time in the critical temperature range (1200° to 800°C) occurs during both the heating and cooling cycle. Secondly a reduction in properties, such as impact toughness, has been observed before sigma precipitates are visible with optical microscopy.

During welding the temperature of the HAZ, several millimetres from the fusion line where sigma usually precipitates, rises and falls with a peak temperature of 850°C to 900°C during the first pass. During subsequent passes the peak temperature decreases on each cycle, although the time at temperature may increase slightly, because welding commences above room temperature (WM&F recommendation is a 70°C –100°C maximum interpass temperature for thin wall pipe). This is for a normal heat input i.e.  $\sim 0.7\text{kJ/mm}$ .

However, when the heat input is excessive and interpass temperatures are too high, the maximum temperature in the HAZ is greater and the time at temperature increases. Calculations show that the width of the depleted zone is about the same if times of 90 seconds at 850°C or 180 seconds at 800°C are used.

Hence the initial use of a time in excess of 60 secs at 900°C seems justified as representative of a series of poor welding cycles which can precipitate sigma phase. This gives a depleted zone width of  $\sim 1\mu\text{m}$  in round figures.

### 3.2 PREN of the Depleted Zone

The simplest way to treat the depleted zone is to take a linear model as shown in Figure 2,

where  $r$  = radius of the sigma particle  
 $R$  = radius of the depleted zone

For the sake of this calculation  $r$  is assumed to be  $1\mu\text{m}$  and  $R = 2\mu\text{m}$ . (i.e. depleted zone width =  $1\mu\text{m}$ ), which appears justified from the work of Francis (2) and the data in Table 3.

The assumption here is that the sigma particles are roughly spherical. However, sigma is usually observed to precipitate in the ferrite at phase boundaries, and this suggests phase boundary diffusion may play a role in the precipitation and growth mechanism. Diffusion along grain and phase boundaries is usually two or more orders of magnitude faster than bulk diffusion (12). However, the narrow width of these boundaries, e.g.  $5 \times 10^{-10}\text{m}$ , means that the process will be limited by diffusion into the boundary from the bulk metal. Hence, although the sigma may be elongated somewhat at phase boundaries, the assumption of a spherical particle is a reasonable first guess.

The extra chromium and molybdenum to form the sigma particle must have come from the surrounding matrix. Hence the shaded areas in Figure 2 are equal. (In this treatment the diffusion of molybdenum is assumed to be similar to that of chromium).

$$\text{i.e. } r \cdot (\text{PREN}_\sigma - \text{PREN}_{\text{parent}}) = \frac{1}{2} \cdot (R-r) \cdot (\text{PREN}_{\text{parent}} - N)$$

$$1 \cdot (58 - 40) = \frac{1}{2} \cdot 1 \cdot (40 - N)$$

$$N = 4$$

where  $N$  = the PREN value of the parent metal at the precipitate interface. Another way to look at this is a sigma particle of radius  $1\mu\text{m}$  surrounded by shells of material of increasing PREN value. Table 4 shows the increasing shell radius with increasing PREN value.

We now need an estimate of the percentage of depleted material necessary to form a continuous network. Using percolation theory it is known (16) that the continuum percolation threshold for a random bi-phase continuum is  $\sim 59\%$  for a 2-D lattice and  $15.7\%$  for a 3-D lattice. Before using these numbers we must justify the underlying assumptions.

The first is that the precipitation of the sigma phase is truly random. Sigma phase in duplex stainless steels forms at phase boundaries, but the grain size and austenite/ferrite spacing is small. Hence, when sigma phase precipitates are seen in the HAZ, the particle spacing is of a similar size to or greater than the phase boundary spacing. This implies that there is little order to the distribution of sigma phase.

Even when the distribution is truly random, the shape of the second phase can affect the critical percolation threshold (16). If the second phase is elongated in any way this will reduce the percolation threshold. A tendency for the second phase to be "blocky" will increase the percolation threshold.

Although sigma particles are roughly spherical, the discussion above suggests that the depleted zones could be elongated along the phase boundaries. A percolation threshold value of 15% has been assumed for the analysis below, but, even if this were reduced to 12%, say, it would not have a significant effect on the conclusions from section 3.3 below. It is from these conclusions that the practical implications of the model arise, and so a detailed evaluation of the exact percolation threshold is unnecessary.

From the above it can be seen that the assumption of 15% for a connected second phase is a reasonable first guess. This must also be true of the depleted zones if corrosion is to propagate. The area of sigma relative to that of the depleted zone can be calculated for different PREN values in the depleted zone as shown in Table 5. Hence it depends how much the PREN value must decrease to lower the corrosion resistance sufficiently for pitting to occur as to how much sigma phase can be tolerated.

In many cases, decreasing the PREN to that of 22 Cr duplex (PREN 34 or 35) is sufficient to cause corrosion, and for this Table 5 shows that about 4% sigma, as particles of 1 $\mu$ m radius, is required.

### 3.3 Effect of Particle Size

The treatment of sigma precipitates so far has assumed a particle diameter of 2 $\mu$ m i.e. at the upper end of the size range reported by Francis (2).

Francis (2) also showed that the much larger precipitates produced by isothermal heat treatment suffered corrosion in the ASTM G48A test, while samples with smaller sigma particles, at the same concentration did not. Francis argued that if the sigma particle is ten times larger, the depleted area around the particle must be 100 times larger. Hence fewer, large particles will give rise to corrosion.

When intermetallics are assessed it is usually by a technique based on the ASTM E562 method. In this any particle is counted where it covers the intersection of two grid lines. This takes no account of particle size, as only the volume fraction is being estimated.

However, if the notional concentration of the particles is the same we can calculate the extent of reduction in the level of large sigma precipitates required to form a continuous network of depleted zones compared to the values in Table 5. The results are shown in Table 6 for large particles 3 times and 5 times bigger than those in Table 5. This assumes that the relationship between the size of the depleted zone and the size of the sigma particle is linear in the unidimensional model.

The growth of the sigma particle and the size of the depleted zone are both controlled by diffusion of chromium and molybdenum, and hence are both a function of  $\sqrt{t}$ , where t is time. At large values of t, the diffusion of more chromium and molybdenum across the depleted zone may distort this relationship, but the assumption of a linear relationship between the size of the sigma particle and the size of the depleted zone appears a reasonable first assumption.

The results show that the critical level of sigma is about 0.5% for a particle three times larger and 0.2% for a particle five times larger. Clearly for smaller sigma particle sizes the critical concentration will be greater than 4%. This demonstrates the high sensitivity of the model to precipitate diameter.

The figures in Table 6 are not dissimilar to those from studies of sigma precipitation showing a large reduction in CPT in the ASTM G48A test over a wide range of sigma concentrations, from 0.3% to 4% (17), presumably covering a range of precipitate sizes.

## 4.0 EXPERIMENTAL DATA

### 4.1 Sea Water

Tests have been conducted in natural sea water flowing at about 0.5 m/sec with 0.5 mg/l chlorine at 35°C, i.e. typical of many sea water piping systems after the heat exchangers.

Six girth welds were exposed in NPS2 schedule 10S pipe. Two welds had been produced with normal heat inputs, two with high heat inputs and the final two with very high heat inputs. After 60 days exposure the pipes were examined for corrosion and microsections were made of corroded areas. The sigma concentrations adjacent to these areas were also evaluated.

Figure 3 shows the maximum depth of attack versus the maximum sigma content. It is possible that the sigma concentration in the corroded areas was greater, but this could not be determined.

These results suggest that the critical concentration of sigma phase in chlorinated sea water at 35°C is about 4% for particles of approximately 1µm radius. With a reduction of the PREN in the depleted zone to 35, corrosion would be expected at this temperature. This agrees well with the model in the previous section.

Tests of this sort are difficult to carry out because of the difficulty of precipitating known quantities of sigma phase when welding. The reason for this is explained by unpublished WM&F research where the sigma concentration was measured for different values of delta T. The results are shown schematically in Figure 4.

Increasing the value of delta T slowly increases the sigma content to about 2 to 2.5%. A slight increase in delta T then produces a large increase in sigma concentration to ~ 5% or more. Hence maintaining a welding parameters envelope so that the sigma content does not exceed 2.5% will produce welds satisfactory for many applications from a corrosion point of view.

It could be argued that once a reasonable amount of corrosion has occurred, the acid conditions in the pit would enable the pit to continue to propagate, and thus a depleted network across the whole sample would be unnecessary. The samples tested in sea water all had their potentials monitored throughout the test. Samples with no corrosion showed potentials of ~ + 600 mV while those which corroded gave potentials of + 600 mV SCE initially which rapidly decreased to between 0 and +100 mV SCE. One sample with 6.3 % sigma showed a potential decrease to ~ 100 mV SCE, but after 20 days it increased to + 600 mV again where it remained throughout the test. This strongly suggests that the pipe had re-passivated and corrosion had stopped. This was probably because the sigma concentration was not sufficient to form a complete network. Hence, a network of depleted zones seems to be required for continuous propagation, at least under the conditions of this test.

## 4.2 Oil and Gas Fluids

In oil and gas fluids the problem of corrosion with super duplex stainless steels is sulphide stress corrosion cracking (SSCC) in sour brines. 22 Cr duplex stainless steel is well known to be more susceptible to SSCC than Zeron 100 and so a drop in PREN to 35 could give a risk of cracking. As for sea water this requires a sigma concentration of about 4% for precipitates of 1µm radius. Francis et al (18) tested Zeron 100 welds with sigma contents up to 2.5% sigma in a sour brine and found no SSCC. However, this is below the 4% sigma "threshold" calculated above.

Pitting in sour brines is not considered a risk except at high temperatures (> 160°C). However, once again 22 Cr duplex is more at risk of pitting than Zeron 100 and so the model again suggests that up to ~ 4% sigma can be tolerated.

In oil and gas fluids low temperature impact toughness is usually required and this often limits sigma concentrations to lower levels. In addition many oil and gas fluids are at high temperature and/or pressure, which means heavy wall pipe is required. The cooling after welding of thicker pipes is generally 3-Dimensional as opposed to 2-Dimensional for thin pipes. 3-D cooling means that the heat can be conducted away from the joint more quickly than with 2-D cooling, and hence sigma precipitation is not generally a problem in thicker pipe (> 7mm), as the welding envelope becomes much more relaxed.

## 4.3 Other Fluids

Flue gas desulphurisation (FGD) slurries often contain high chlorides as well as sulphates, with oxidising ions such as Fe<sup>3+</sup> and partially oxidised sulphur species, at pH's from 4 to 6 (19). Francis (19) showed that a cast 25 Cr duplex stainless steel showed a much lower critical crevice temperature than that of cast Zeron 100 in two different synthetic slurry solutions. The PREN of the cast 25 Cr duplex was 36 and hence the 4% sigma figure (for particles of 1µm radius) also seems to be justified in this case.

However, in mineral acids, or strongly acidic brines, it is known that, in addition to chromium and molybdenum, copper and tungsten also play a part in the corrosion resistance. These elements have not been evaluated in the present analysis and it is possible that in this case the figure of 4% sigma phase may be too high.

## 5.0 RECOMMENDATIONS

The discussion in section 3.3 shows that the particle size strongly affects the critical sigma concentration for corrosion to occur. The present method of evaluating sigma concentrations from microsections (based on ASTM E562) does not take this into account. Also the unpublished TWI work (13) shows that the temperature of sigma phase formation can also affect the subsequent corrosion behaviour.

Hence it is recommended that welds be evaluated with fitness for purpose tests. These should be:-

- 1) A low temperature impact toughness test: where toughness at low temperatures is required (e.g. oil and gas projects).

- 2) A corrosion test: this can be an ASTM G48A test, an autoclave test, or an electrochemical test, as may be deemed appropriate.

Note that all of the above commentary is related only to welds and weld zones and not parent metal.

## **6.0 CONCLUSIONS**

- 1) A simple model has been developed for the critical concentration of sigma particles in the HAZ of welds to cause corrosion problems.
- 2) This model correlates well with experimental data from chlorinated sea water exposure.
- 3) The model shows that sigma particle size is the most critical factor, and yet this is not accounted for in current methodologies for sigma evaluation.
- 4) The use of impact toughness tests and corrosion tests is preferred to the assessment of sigma concentration by metallography and point counting.

## **ACKNOWLEDGEMENTS**

The author would like to thank Dr. R. Todd of the Materials Department, UMIST, Professor R. Newman of the Corrosion and Protection Department, UMIST and Dr. T. G. Gooch of TWI for the helpful discussions during the formulation of the ideas in this report.

## REFERENCES

1. A. J. Strutt - Ph.D Thesis, University of Manchester, 1987.
2. R. Francis Discussion Brit. Corr. J. 27, 4 (1992) 319.
3. B. Weiss and R. Stickler, Metallurgical Transactions, Vol.3, p.851 1972.
4. J.K. Lai, Materials Science and Engineering, Vol.49, p.19. 1981
5. G. Herbsleb and P. Schwaab, Duplex Stainless Steels Conference Proceedings, ASM Metals/Materials Technology Series, Paper. St. Louis USA. (8201-002) p.15 1982.
6. G. F. Slattery, S.R. Keown and M.E. Lambert, Metals Technology Vol.10,p.373 1983.
7. J.K. Lai, D.J. Chastell and P.E.J. Flewitt, CEGB Report RD/L.N 97/80 1980.
8. J. Chance, K.J. Gradwell, W.Coop and C.V. Roscoe, Duplex Stainless Steels Conference Proceedings, ASM Metals/Materials Technology Series, Paper (8201-019) p.371 1982. St. Louis, USA.
9. C.V. Roscoe, "The Phase Transformations of Duplex Stainless Steel Casting Alloys", M.Sc. Thesis, University of Manchester, 1981.
10. T. Thorvaldsson, H. Eriksson, J.Kutka and A. Salwen, Stainless Steels '84 Proceedings of Göteborg Conference, Book No. 320, The Institute of Metals, 1 Carlton House Terrace, London SW1Y 5DB. p.101 1985.
11. C.V. Roscoe. PhD Thesis, University of Manchester, 1987.
12. I. Kaur and W. Gust Handbook of Grain and Interface Boundary Diffusion Data. Publ<sup>d</sup>. by Ziegler Press, Stuttgart 1989.
13. B J Ginn and T G Gooch "Effect of intermetallic content on pitting resistance of ferritic/austenitic stainless steels"; Stainless Steel '99, Associazione Italiana di Metallurgia, Chia Laguna, Sardinia Italy; June 1999
14. C. Strawström and M. Hillert. JISI 207 (1969) 77.
15. J. Charles. Duplex Stainless Steels 1991. Beaune, France Oct. 1991 - les editions de physique, page 3
16. R. Zallen, The Physics of Amorphous Solids. J. Wiley and Sons 1983; Page 183-191

17. T. G. Gooch. The 1995 Comfort A. Adams Lecture (AWS)  
Welding Journal 75, 5 (1996) 135-S
18. R. Francis - Paper 12 - Corrosion '97, New Orleans USA March 1997, NACE.
19. R. Francis - Paper 479 - Corrosion '98 San Diego, USA March 1998, NACE.

**TABLE 1 Composition of the sigma phase in 25Cr duplex stainless steel**

| COMPOSITION (wt%) |      |      |     | PREN* | Ref |
|-------------------|------|------|-----|-------|-----|
| Fe                | Cr   | Mo   | Ni  |       |     |
| 55.0              | 29.0 | 11.0 | 5.0 | 65.3  | 3   |
| 53.3              | 36.9 | 4.1  | 4.9 | 50.4  | 4   |
| Bal               | 28.8 | 7.5  | 3.3 | 53.6  | 5   |
| 56.6              | 28.0 | 8.2  | 5.0 | 55.1  | 6   |
| 44.0              | 29.0 | 8.0  | -   | 55.4  | 7   |
| 47.8              | 30.8 | 9.7  | 4.2 | 62.8  | 8   |
| 50.5              | 28.0 | 10.8 | 3.7 | 63.6  | 9   |
| 56.6              | 29.5 | 9.6  | 3.1 | 61.2  | 10  |
| 51.0              | 32.0 | 8.0  | 3.2 | 58.4  | 11  |
| MEAN              |      |      |     | 58    |     |

Bal = balance

\*PREN = % Cr + 3.3%Mo + 16%N

**TABLE 2 Diffusion coefficients for chromium  
and nickel in stainless steel (Ref 12)**

| ALLOY        | SPECIES | PHASE   | VOLUME DIFFUSION       |                |                         |                    |
|--------------|---------|---------|------------------------|----------------|-------------------------|--------------------|
|              |         |         | $D_0$<br>( $m^2/sec$ ) | Q<br>(kJ/mole) | TEMP<br>( $^{\circ}C$ ) | D<br>( $m^2/sec$ ) |
| Unkown       | Cr      | Aust.   | 3.70E-05               | 280            | 800                     | 8.65E-19           |
|              |         |         | 3.70E-05               | 280            | 900                     | 1.26E-17           |
|              |         |         | 3.70E-05               | 280            | 1000                    | 1.20E-16           |
|              | Cr      | Ferrite | 2.00E-04               | 251            | 800                     | 1.21E-16           |
|              |         |         | 2.00E-04               | 251            | 900                     | 1.33E-15           |
|              |         |         | 2.00E-04               | 251            | 1000                    | 1.00E-14           |
| Fe/16Cr/14Ni | Cr      | Aust.   | 6.00E-06               | 175.7          | 800                     | 1.68E-14           |
|              |         |         | 6.00E-06               | 175.7          | 900                     | 8.99E-14           |
|              |         |         | 6.00E-06               | 175.7          | 1000                    | 3.70E-13           |
|              | Ni      | Aust.   | 1.80E-05               | 278            | 800                     | 5.27E-19           |
|              |         |         | 1.80E-05               | 278            | 900                     | 7.50E-18           |
|              |         |         | 1.80E-05               | 278            | 1000                    | 7.04E-17           |

$D_0$  = Diffusion constant

Q = Activation energy

D = Diffusion coefficient

**TABLE 3 Width of the depleted zone around sigma phase precipitates as a function of time and diffusion coefficient**

| <b>TIME<br/>(sec)</b> | <b>DIFF. COEFF.<br/>(m<sup>2</sup>/sec)</b> | <b>WIDTH<br/>(µm)</b> |
|-----------------------|---|-----------------------|
| 10                    | 1.00E-17                                    | 0.0                   |
| 10                    | 1.00E-16                                    | 0.1                   |
| 10                    | 1.00E-15                                    | 0.2                   |
| 10                    | 1.00E-14                                    | 0.6                   |
| 30                    | 1.00E-17                                    | 0.0                   |
| 30                    | 1.00E-16                                    | 0.1                   |
| 30                    | 1.00E-15                                    | 0.3                   |
| 30                    | 1.00E-14                                    | 1.1                   |
| 60                    | 1.00E-17                                    | 0.0                   |
| 60                    | 1.00E-16                                    | 0.2                   |
| 60                    | 1.00E-15                                    | 0.5                   |
| 60                    | 1.00E-14                                    | 1.5                   |
| 120                   | 1.00E-17                                    | 0.1                   |
| 120                   | 1.00E-16                                    | 0.2                   |
| 120                   | 1.00E-15                                    | 0.7                   |
| 120                   | 1.00E-14                                    | 2.2                   |
| 240                   | 1.00E-17                                    | 0.1                   |
| 240                   | 1.00E-16                                    | 0.3                   |
| 240                   | 1.00E-15                                    | 1.0                   |
| 240                   | 1.00E-14                                    | 3.1                   |

\* - From Strawstrom and Hillert equation (Ref 14)

**TABLE 4 Radius of the depleted zone for varying PREN values for a 1µm radius sigma particle**

| <b>PREN*</b> | <b>RADIUS<br/>(µm)</b> |
|--------------|------------------------|
| 10           | 1.17                   |
| 15           | 1.31                   |
| 20           | 1.44                   |
| 25           | 1.58                   |
| 30           | 1.72                   |
| 35           | 1.86                   |
| 40           | 2.00                   |

\*PREN = %Cr + 3.3% Mo + 16%N

**TABLE 5 Critical sigma concentration for 15% depleted zones for different PRENS for sigma particles of 1µm radius**

| <b>PREN*</b> | <b>FRACTIONAL AREA +</b> | <b>SIGMA CONTENT (%)</b> |
|--------------|--------------------------|--------------------------|
| 10           | 1.4                      | 10.7                     |
| 15           | 1.7                      | 8.8                      |
| 20           | 2.1                      | 7.1                      |
| 25           | 2.5                      | 6.0                      |
| 30           | 3.0                      | 5.0                      |
| 35           | 3.5                      | 4.3                      |
| 40           | 4.0                      | 3.8                      |

\* PREN + %Cr + 3.3%Mo + 16%N

+ Fractional Area = (Area depleted zone) / (Area sigma)

**TABLE 6 Sigma particle concentration for  
15 vol% continuous depleted zone for  
several particle sizes**

| PREN* | SIGMA CONCENTRATION (%) |      |      |
|-------|-------------------------|------|------|
|       | DIAMETER (μm)           |      |      |
|       | 2                       | 6    | 10   |
| 25    | 6.0                     | 0.67 | 0.24 |
| 30    | 5.0                     | 0.56 | 0.20 |
| 35    | 4.3                     | 0.48 | 0.17 |
| 40    | 3.8                     | 0.48 | 0.15 |

\*PREN = %Cr + 3.3% Mo + 16%N

**FIGURE 1 Comparison between sigma phase formation under TTT and CCT conditions in forged Zeron 100 (Ref 1)**

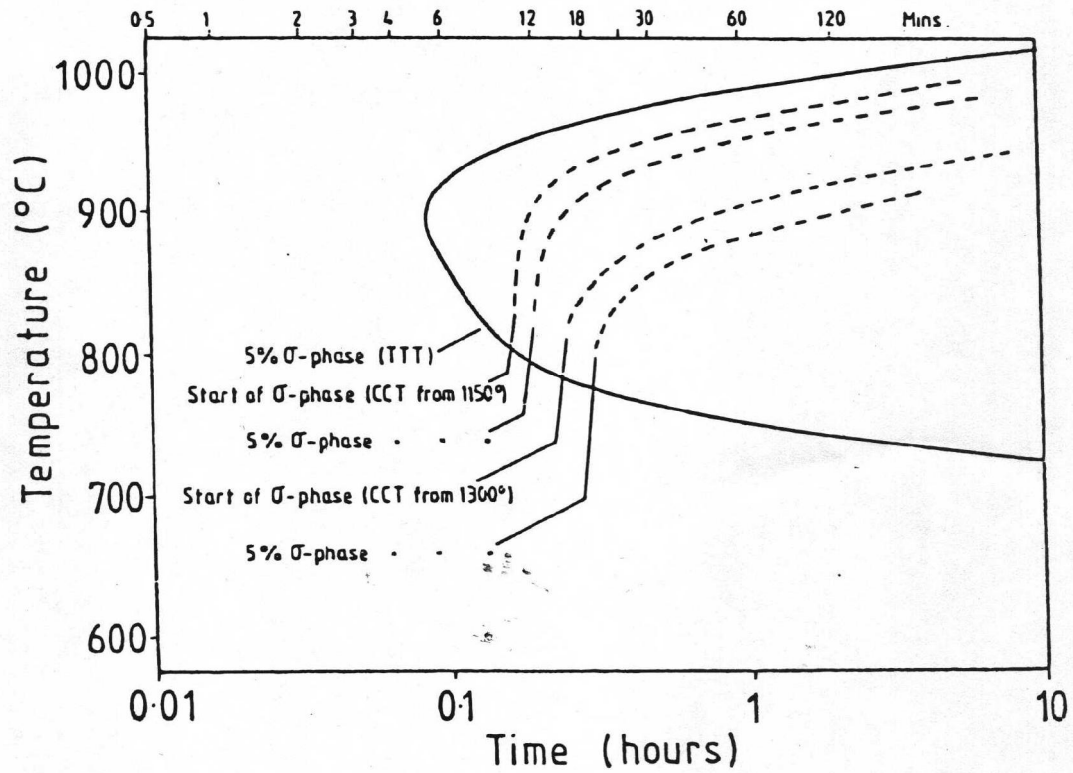


**FIGURE 2 Schematic diagram of PREN at sigma particle and depleted zone**

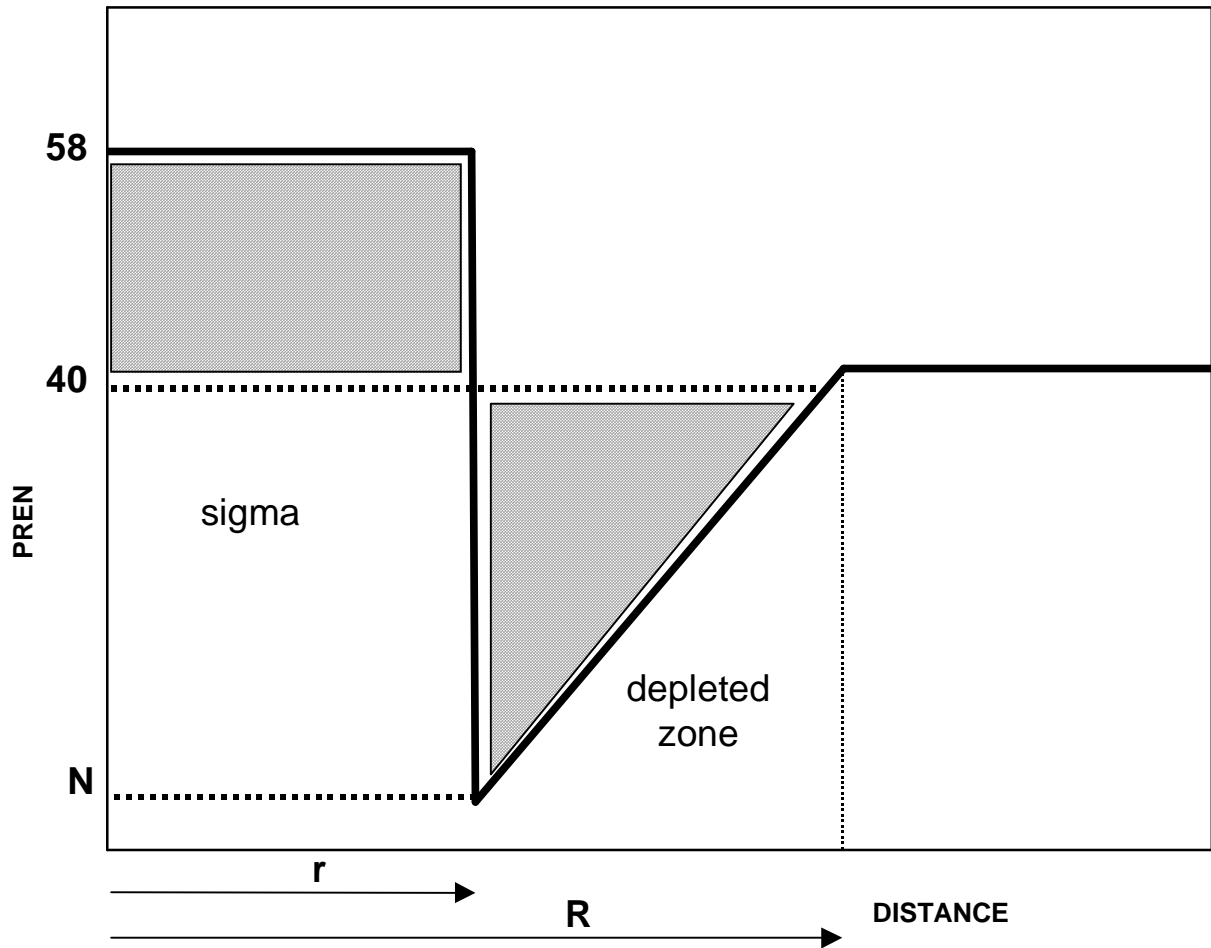


**FIGURE 3 Depth of attack versus sigma content in chlorinated sea water at 35°C**

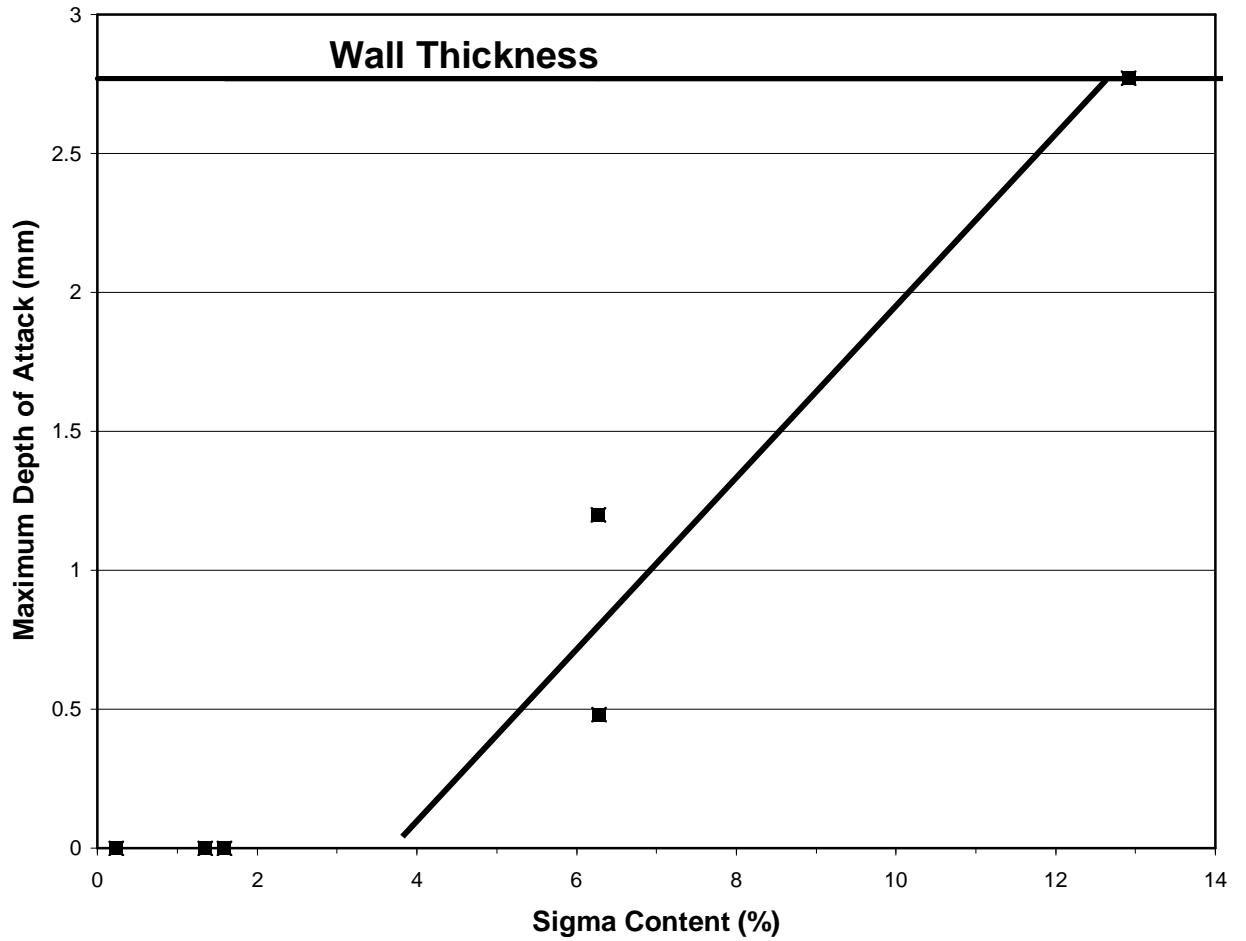


**FIGURE 4 Schematic diagram of sigma precipitation versus delta T (1200-800°C)**

